5
Targets

In this chapter we will briefly review the various types of targets used in particle physics experiments. The target normally consists of a piece of metal or liquid hydrogen. However, a number of other types of targets are sometimes used in specialized applications. These include polarized targets for spin dependent measurements, gas jets, active targets, and beam dumps.

5.1 Standard targets

Most particle physics experiments at fixed target accelerators use either a thin metal target or a cryogenic target containing liquid hydrogen or deuterium. The choice of target is dictated by considerations of the required signal rate, associated background, and necessary resolution. The finite target size and absorption, energy degradation, and multiple scattering in the target can all affect the measurement resolution.

The chief advantages of metal targets are the high interaction rate and the convenience of preparation. Solid targets such as beryllium are widely used in experiments studying muon production. A disadvantage is the amount of multiple scattering and absorption suffered by particles produced in the block. This can have a deleterious effect on experiments studying the effective mass of produced hadrons. The extraction of nucleon cross sections from scattering data with a nuclear target usually involves some sort of model-dependent or background target subtraction.

Liquid hydrogen targets offer the best resolution for the study of hadronic resonances. The multiple scattering and nuclear absorption are small. On the other hand, the density of liquid hydrogen is only 0.070 g/cm^3, so that the interaction rate per incident beam particle ($\sim 4 \times 10^{-6}/\mu$b-m) is smaller than that obtained with a solid target. Since

the normal boiling point of H_2 is 20 K, the target requires an associated cryogenic system. Liquid deuterium with a density of 0.16 g/cm^3 and normal boiling point of 24 K can be used to study interactions involving neutrons. Some properties of common cryogenic fluids are given in Table 5.1.

A typical liquid hydrogen or deuterium target contains a cylinder along the beam path to hold the cryogenic fluid [1]. Figure 5.1 shows a schematic of a liquid hydrogen target. The beam enters and leaves the target through a mylar or other thin window. The cylinder is surrounded by an insulating jacket. The target gas is precooled in heat exchangers and liquified by passing the cooled gas through an expansion valve. The hydrogen density and liquid level are carefully monitored. Calibration runs with the target empty are used to determine the rate or characteristics of events coming from the target assembly.

All targets other than hydrogen have complications due to Fermi momentum and nuclear shadowing. The Fermi momentum is due to the continual motion of the nucleons inside the nucleus. It is possible to make a rough estimate of the magnitude of this momentum for various nuclei [2]. Two identical nucleons may not occupy the same energy level. Since they must obey Fermi statistics, the number of occupied states with mo-

Table 5.1. *Properties of cryogenic liquids at NBP*

	Melting point at 1 atm (K)	Normal boiling point at 1 atm (K)	Density (g/cm^3)	Heat of vaporization (J/g)	Specific heat (J/g-K)	Thermal conductivity (mW/cm-K)
^{3}He	[a]	3.19	0.059	11[b]	3.3[c]	0.20
^{4}He	[a]	4.215	0.125	21.7	4.50	0.27
H_2	14.0	20.4	0.070	447	9.5	1.19
D_2	18.7	23.6	0.163	304	5.8[d]	1.34
Ne	24.5	27.1	1.20	86.1	1.85	1.13
N_2	63.3	77.3	0.807	199	2.05	1.38
Ar	84.0	87.3	1.39	163	1.14	1.22

[a] Does not solidify at 1 atm.
[b] At 3.0 K.
[c] At 2.4 K.
[d] At 22 K.
Source: R. Scott, *Cryogenic Engineering,* Princeton: Van Nostrand, 1959; B. Colyer, Cryogenic properties of ^{3}He and ^{4}He, Rutherford Laboratory report RHEL/R138, 1966; T. Roberts and S. Sydoriak, Phys. Rev. 98: 1672, 1955; G. Haselden (ed.), *Cryogenic Fundamentals,* New York: Academic Press, 1971.

Figure 5.1 Schematic diagram of a liquid hydrogen target. (1) Liquid nitrogen supply, (2) hydrogen gas return, (3) hydrogen gas supply, (4) nitrogen gas return, (5) insulating vacuum, (6) heat exchanger, (7) liquid nitrogen reservoir, (8) expansion valve, (9) liquid hydrogen reservoir, (10) valve, (11) level indicator, and (12) thin windows.

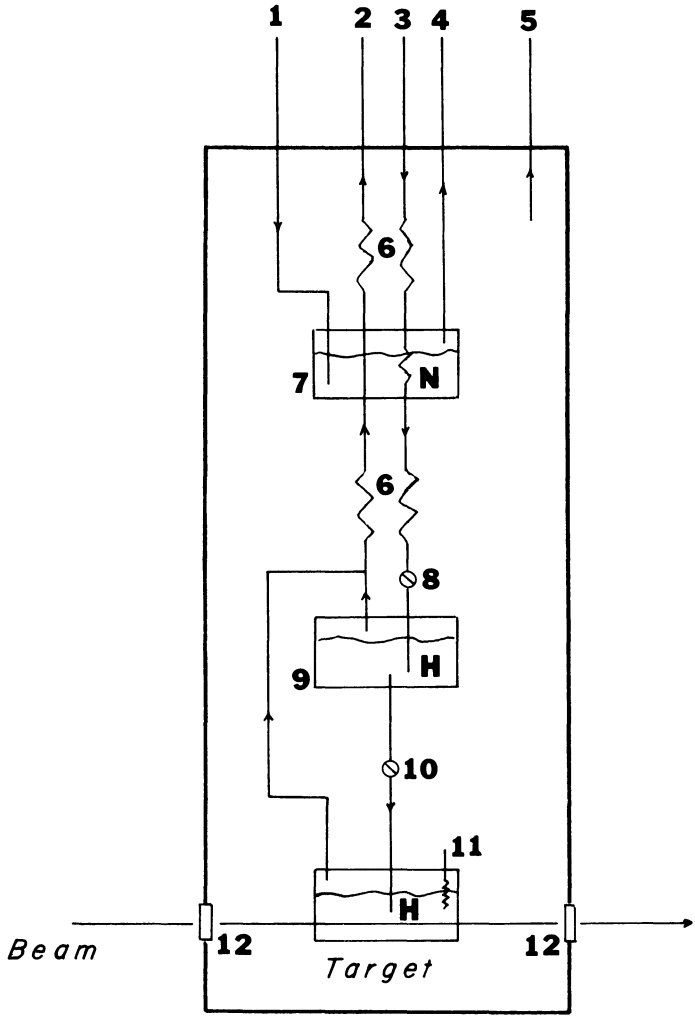

mentum less than p is

$$\frac{1}{h^3} 2 \frac{4}{3} \pi r_n^3 \frac{4}{3} \pi p^3$$

Thus, for a nucleus with Z protons and $A-Z$ neutrons we have

$$\begin{aligned} \frac{2}{h^3} \frac{4}{3} \pi r_n^3 \frac{4}{3} \pi p_p^3 &= Z \\ \frac{2}{h} \frac{4}{3} \pi r_n^3 \frac{4}{3} \pi p_n^3 &= A - Z \end{aligned} \tag{5.1}$$

For heavy nuclei the Fermi momentum of neutrons is substantially larger than that of protons.

Figure 5.2 shows the measured Fermi momentum in deuterium. The calculated momentum peaks at approximately 50 MeV/c and has a high momentum tail extending beyond 200 MeV/c. The peak momentum in carbon is around 150 MeV/c. The Fermi momentum can have an appre-

Figure 5.2 Spectator momentum distribution for protons in deuterium. The curve follows from the potential model of T. Hamada and I. Johnston, Nuc. Phys. 34: 382, 1962. The data deviate from the curve at small momenta due to bubble chamber scanning losses. (R. Fernow, unpublished data.)

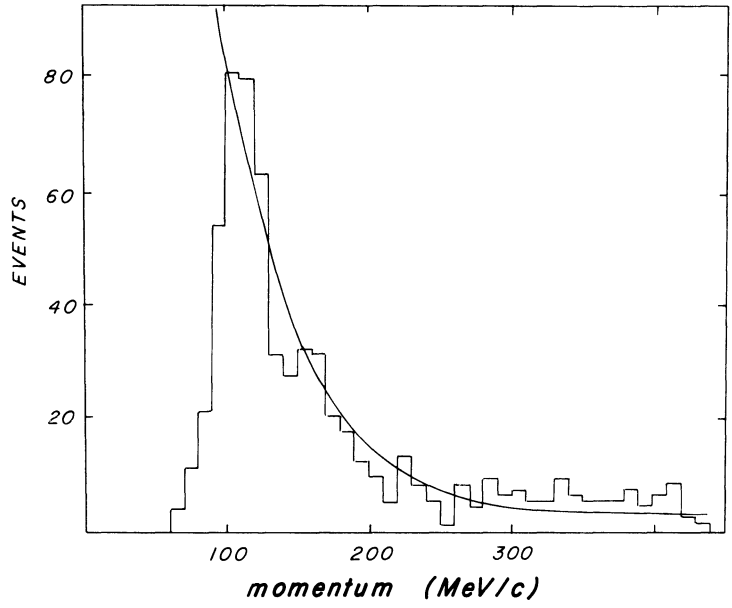

ciable effect on the kinematics of particle reactions. Interactions with a fixed beam momentum occur over a spectrum of CM energies. Uncertainty of the momentum of the target nucleon leads to a loss of resolution compared to interactions in hydrogen.

The second complication in nonhydrogen targets is nuclear shadowing [3]. Consider a high energy beam incident on a nuclear target. To the lowest-order approximation the nucleus appears as an assemblage of free nucleons. However, because of the finite probability of being absorbed in the nucleus, a beam particle is more likely to interact with the first nucleon it encounters rather than with a nucleon on the opposite side of the nucleus. Thus, the first target nucleons cast a "shadow" that reduces the probability of an interaction in the nucleus below the sum of the individual nucleon probabilities. Crudely, the shadowing effect in deuterium gives rise to the relation

$$\sigma_{\mathrm{d}} = \sigma_{\mathrm{n}} + \sigma_{\mathrm{p}} - \frac{1}{4\pi}\,\sigma_{\mathrm{n}}\sigma_{\mathrm{p}}\left\langle \frac{1}{r_{\mathrm{d}}^2} \right\rangle \tag{5.2}$$

where r_{d}^2 is the mean square distance between the neutron and proton in the deuteron ground state. Other effects present in nuclear targets include scattering off more than one nucleon, and combinations of scattering and absorption.

5.2 Special purpose targets

In this section we will discuss several types of targets that are used for special applications. Some experiments use an active target, meaning that the target medium is also a detector. The classic example of this is a bubble chamber. Counter neutrino experiments frequently employ liquid scintillator or segmented calorimeter targets. Experiments to measure the properties of short-lived states have used finely divided solid state detectors as targets.

Bellini et al. [4] have used a telescope made up from 40 silicon detectors, each with a thickness of 300 μm and separated from each other by 150 μm. A minimum ionizing particle deposits about 80 keV in each layer. The signal from each layer was amplified, shaped, and measured with an analog to digital converter. Figure 5.3 shows schematically the output from the layers, expressed as an equivalent number of minimum ionizing particles. The sudden jumps in the output by two equivalent particles are assumed to arise from the decays of two short-lived charged particles into three charged body decay modes.

At the opposite extreme from the active targets are beam dump experiments in which the beam is directed into a large mass of absorber [5]. Here the object is to quickly absorb normal hadrons near the interaction point. In that case muons or other particles emerging from the dump are more likely to be directly produced in the interaction and not result from the decay of ordinary hadrons.

A gas jet target delivers a narrowly collimated beam of gas. It is normally used inside the main accelerator ring. At predetermined times during the acceleration cycle a pulse of gas is directed into the circulating beam. Two advantages of a gas jet target are (1) the low gas density permits very low energy recoil particles to escape the interaction area and be detected and (2) the resolution on the measurement of the energy of the circulating incident beam is extremely good. The Fermilab gas target [6] has an equivalent thickness of only 4×10^{-7} g/cm^2. The jet has a $\pm$ 3-mm width and a 100-ms pulse length. The primary difficulty arising from the use of such targets is the background gas introduced into the

Figure 5.3 Schematic representation of the output from the active silicon target of Bellini et al. [4] for an event with two decaying particles.

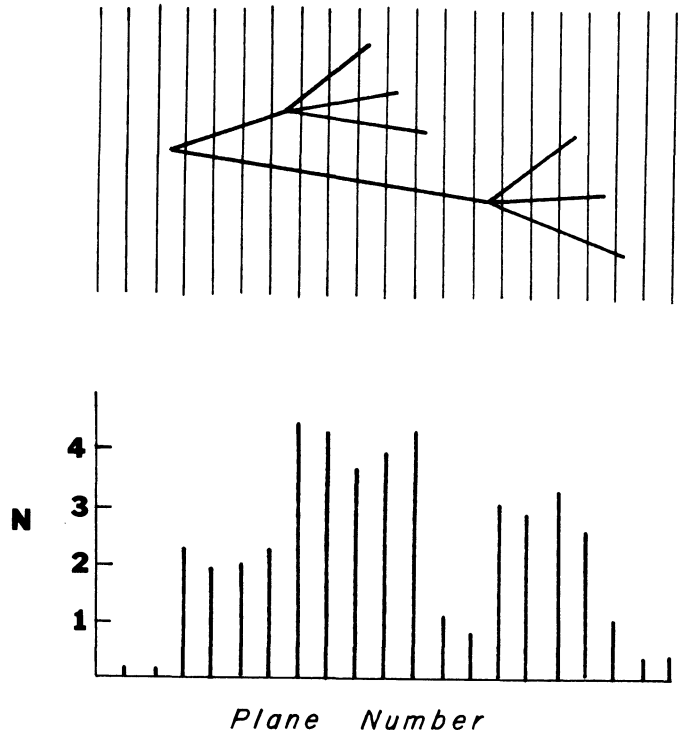

accelerator beam pipe. Large systems of diffusion pumps are necessary to reduce the gas pressure in the vicinity of the interaction point.

Polarized proton and deuteron targets are used in the study of the spin dependence of particle interactions [7]. A schematic of a polarized target system is shown in Fig. 5.4. The target contains five major subsystems: (1) the actual target material, (2) a cryogenic system, (3) a magnetic field, (4) a microwave system, and (5) a nuclear magnetic resonance (NMR) system. Polarized targets operate with magnetic fields above 2.5 T and at temperatures below 1 K. The low temperature can be achieved with ^{4}He or ^{3}He evaporation cryostats or with a dilution refrigerator.

Figure 5.4 Schematic diagram of the target region in a horizontal evaporation cryostat for a polarized proton target. (A) Magnet pole tip, (B) end of the cryostat, (C) ^{3}He fill line, (D) microwave guide, (E) Teflon seal, (F) copper cavity, (G) NMR coil, (H) NMR cable, (J) target beads, and (K) returning ^{3}He gas.

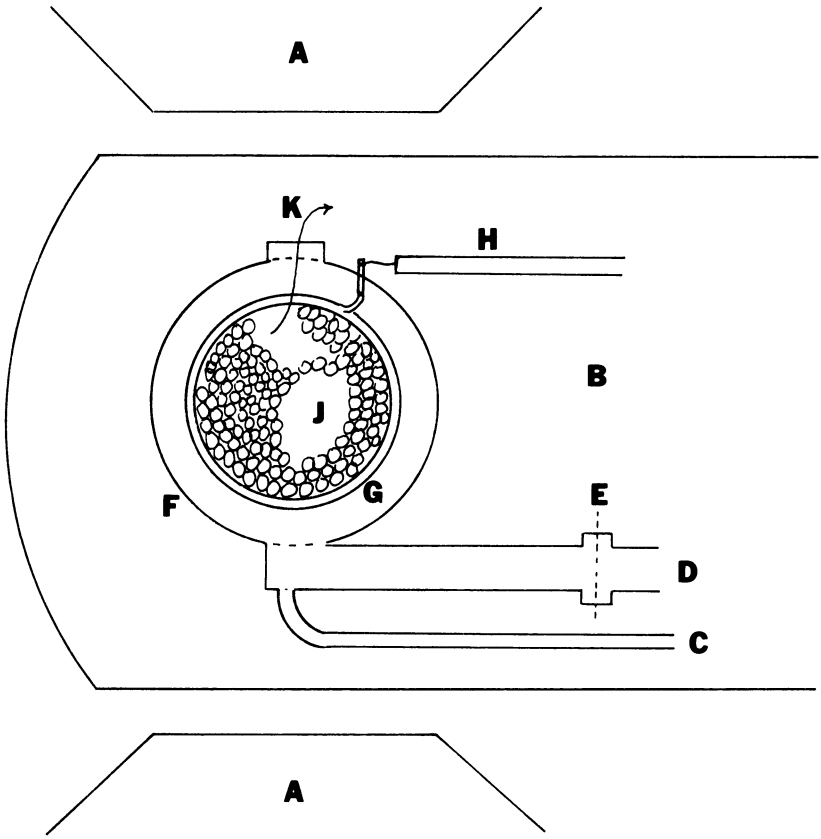

The actual target material consists of frozen beads of compounds, such as ammonia, butanol, or propanediol, which have been doped with a small proportion of a paramagnetic substance. The hydrogen atoms in the target provide the material to be polarized. Under the conditions of high magnetic field and low temperature, the free electrons in the paramagnetic additive are easily polarized to nearly 100%. Because of its much smaller magnetic moment, the proton polarization under the same conditions is $<1\%$. However, if microwaves of the proper frequency are radiated into the target mixture, the electron and proton spin systems become coupled, and it is possible to transfer substantial polarization to the protons. The magnitude of the polarization is usually determined by surrounding the target material with a coil and measuring the voltage change caused by the nuclear magnetic resonance of the polarized protons.

References

[1] G. Janes, Target preparation, in D. Ritson (ed.), *Techniques of High Energy Physics,* New York: Interscience, 1961, Chap. 10.
[2] B. Rossi, *High Energy Particles,* Englewood Cliffs: Prentice-Hall, 1952.
[3] V. Franco and R. Glauber, High energy deuteron cross sections, Phys. Rev. 142: 1195–1214, 1966.
[4] G. Bellini, P. D'Angelo, P. Manfredi, E. Meroni, L. Moroni, C. Palazzi Cerrina, F. Ragusa, and S. Sala, Active target for lifetime measurements of charmed particles and related signal processing, Nuc. Instr. Meth. 196: 351–60, 1982.
[5] R. Ball, C. Coffin, H. Gustafson, M. Crisler, J. Hoftun, T. Ling, T. Romanowski, J. Volk, S. Childress, M. Duffy, G. Fanourakis, R. Loveless, D. Reeder, D. Schumann, E. Smith, L. Jones, M. Longo, T. Roberts, B. Roe, E. Wang, C. Castoldi, and G. Conforto, Prompt muon-neutrino production in a 400 GeV proton beam dump experiment, Phys. Rev. Lett. 51: 743–6, 1983.
[6] A. Bujak, P. Devensky, A. Kuznetsov, B. Morozov, V. Nikitin, P. Nomokonov, Y. Pilipenko, V. Smirnov, E. Jenkins, E. Malamud, M. Miyajima, and R. Yamada, Proton-helium elastic scattering from 45 to 400 GeV, Phys. Rev. D 23: 1895–1910, 1981.
[7] See, for example, the reports in G. Bunce (ed.), *High Energy Spin Physics—1982,* New York: AIP, AIP Conf. Proc. No. 95, 1982, pp. 464–533.

Exercises

1. Compare the interaction rates per unit cross section, multiple scattering, and energy loss for a 5-GeV/c K^- beam incident on 20-cm-long liquid hydrogen, beryllium, and copper targets.
2. Estimate the Fermi momentum of the neutrons and protons in lead.
3. What is the maximum difference in CM energies for 20-GeV/c protons incident on deuterium due to Fermi momentum?